Hardware development for Gravity Probe-B

D. Bardas, W. S. Cheung, D. Gill, R. Hacker, G. M. Keiser,
J. A. Lipa, M. Macgirvin, T. Saldinger, J. P. Turneaure, M. S. Wooding
Stanford University

J. M. Lockhart
Stanford University and San Francisco State University

Relativity Gyroscope Program, Hansen Laboratories,
Stanford University, Stanford, California 94305

Abstract

Gravity Probe-B (GP-B), also known as the Stanford Relativity Gyroscope Experiment, will test two fundamental predictions of Einstein's General Theory of Relativity by precise measurement of the precessions of nearly perfect gyroscopes in earth orbit. This endeavor will be the result of over 25 years of research and embodies state-of-the-art technologies in many fields including, among others, gyroscope fabrication and readout, cryogenics, superconductivity, magnetic shielding, precision optics and alignment methods, and satellite control systems. These technologies are necessary to enable measurement of the predicted precession rates to the milli-arcsecond/year level and to reduce to "near zero" all non-General Relativistic torques on the gyroscopes. This paper, the first of six on GP-B at this conference, will provide a brief overview of the experiment followed by descriptions of several specific hardware items with highlights on progress to date and plans for future development and tests.

Overview of the experiment

In 1960 L. I. Schiff[1,2] suggested a new test of General Relativity based on the measurement of the precession of a gyroscope in earth orbit. Shown schematically in Figure 1 are the two relativistic precession rates, measured with respect to inertial space, for a

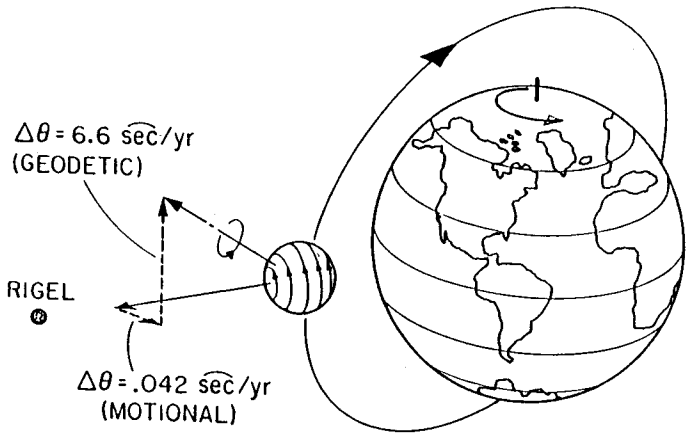

Figure 1. Relativistic effects as seen in gyroscope with spin vector oriented as shown and lying parallel to the line of sight to Rigel.

gyroscope in free fall about a rotating massive sphere. These precession rates correspond to the two terms in the following formula which Schiff derived from the equations of General Relativity:

$$\underline{\Omega} = \frac{3}{2}\frac{GM}{c^2R^3}(\underline{R}\times\underline{v}) + \frac{GI}{c^2R^3}\left[\frac{3\underline{R}}{R^2}(\underline{\omega}\cdot\underline{R}) - \underline{\omega}\right] \qquad (1)$$

where $\underline{R}$ and $\underline{v}$ are the instantaneous position and velocity of the gyroscope relative to the center of the rotating body, and M, I, and $\underline{\omega}$ are the mass, moment of inertia and angular velocity of the central body, in this case the Earth. The first term in equation (1) is the geodetic precession rate, Ω_G, resulting from the motion of the gyroscope through curved space-time around the earth, and the second term, Ω_M, is the motional (also known as the

gravitomagnetic) precession rate resulting from the rotation of the Earth. In a near-circular polar orbit of altitude 650 kilometers, the geodetic and motional precession rates are orthogonal to each other and have time-averaged values of 6.6 and 0.042 arcsecond/year, respectively. In practice, the precession of the gyroscope will be measured with respect to the line of sight to a suitable guide star (Rigel) with appropriate data reduction to account for the star's proper motion and any difference between its actual and apparent position.

With extreme care taken to minimize all other possible torques on the gyroscopes, so that their resultant contribution to the drift rate is less than ~ 0.3 milli-arcsecond/year, we expect a GP-B Science Mission of 1 to 2 years to yield a determination of the relativity effects with a precision of better than 2 parts in 10^4 for Ω_G and better than 2 percent for Ω_M. The experiment will also test two smaller precession predictions of General Relativity and, in addition, it will provide a new check of the relativistic deflection of starlight, and the potential to improve our understanding of the nearby distance scale of the universe. A discussion of these is beyond the scope of this paper; however details of these, as well as the historical and scientific background to the experiment, are presented by Everitt[3]. Whether or not the experiment verifies the predicted geodetic and/or motional precession rates calculated by Schiff, it will doubtless stimulate a more comprehensive understanding of gravitational forces and astrophysical phenomena. Additional dividends of the experiment are already forthcoming in the form of technology improvements in a number of scientific disciplines.

The concept for the Relativity Gyroscope Experiment is simple. The difficulty lies only in attaining the precision needed. Doing a 1 milli-arcsecond/year experiment requires a gyroscope with an absolute drift rate of about 10^{-11} deg/hr (equivalent to $\sim 5 \times 10^{-17}$ rad/second or ~ 0.3 milli-arcsecond/year), some nine orders of magnitude better than current inertial navigation gyroscopes. In addition, the precision needed for line-of-sight determination to Rigel places severe design requirements on the telescope, its readout, and its attachment to the gyroscope reference structure. Several fundamental requirements have been identified[3,4] for success of the experiment and are discussed in an accompanying paper by Young[5]. All but one of these requirements concern instrument precision and/or experimental method and are under our control. However, one requirement is an adequate knowledge of the proper motion of Rigel whose present uncertainty of 1.7 milli-arcsecond/year in right ascension represents the largest expected error in the experiment. A more accurate value for the proper motion of Rigel is expected to be determined by the time of the GP-B Science Mission, or shortly thereafter and, if necessary, can be included in post experiment data analysis. Van Patten et al.[6] describe the data extraction scheme for GP-B in an accompanying paper.

The gyroscope

Before describing the configuration of the complete instrument, we discuss the main elements of the gyroscope. An exploded isometric view of the gyroscope is shown in Figure 2. The gyroscope consists of an extremely spherical and homogeneous fused quartz rotor, approximately 1.5 inch in diameter, spinning within a fused quartz housing. Each housing half

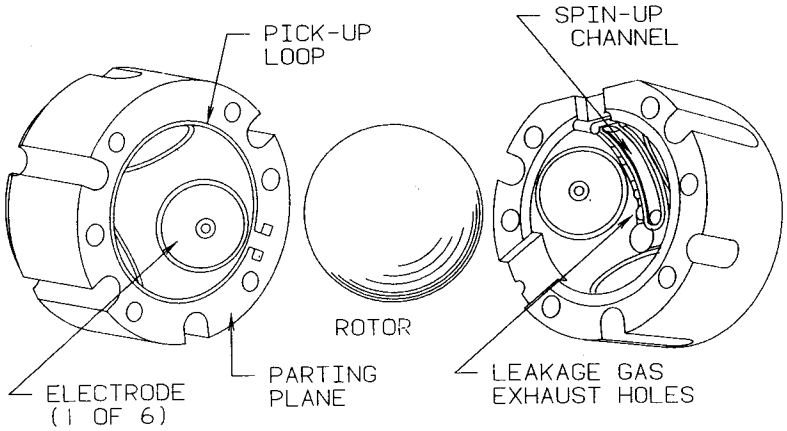

Figure 2. Exploded view of gyroscope.

consists of a hemispherical cavity which forms a spherical enclosure around the rotor when assembled so that the respective parting planes are touching. The surface of the rotor is coated with a very thin and uniform layer of niobium, which is superconducting at the

operating temperature (~2K) of the experiment. (The superconducting transition temperature of niobium is 9.2K). This superconducting layer is essential for two reasons: 1) it allows the rotor to be suspended electrostatically[7,8] within its fused quartz housing by voltages applied to a set of 3 mutually orthogonal pairs of suspension electrodes with nominal clearance to the rotor surface of 0.001 inch; 2) it provides the physical basis for precise readout of gyroscope drift. This latter point provides one of several reasons that the experiment must be conducted at cryogenic temperatures. Other justifications for operation at cryogenic temperatures will be discussed later in this paper.

The method of gyroscope readout is shown schematically in Figure 3. A rotating superconducting shell developes a London[9] magnetic moment, M_L, when spun up below its superconducting transition temperature. The effects of this magnetic moment are externally equivalent

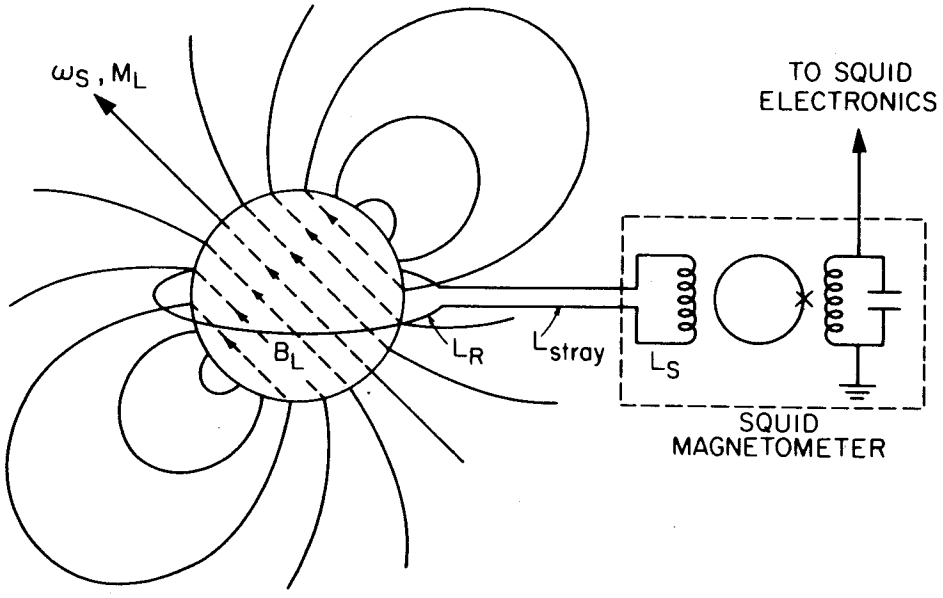

Figure 3. Superconducting gyroscope readout system.

to those of a magnetic field, $B_L = 1.14 \times 10^{-7}\ \omega_S$ gauss (where ω_S is the spin angular velocity of the rotor), which is uniform inside the rotor and exactly aligned with the spin axis. The rotor is encircled by a thin film superconducting pick-up loop (located on the parting plane of the gyroscope as in Fig. 2) which serves to couple the magnetic flux from the rotor to a SQUID (Superconducting QUantum Interference Device) flux-to-voltage converter. In practice the pick-up loop will consist of multiple turns, for optimum flux coupling, but for clarity these are not shown here. A change in the direction of the rotor spin axis will change the magnetic flux intercepted by the loop and hence changes the current in the SQUID input circuit. A more detailed discussion of this readout scheme is given in an accompanying paper by Lockhart[10].

The rotor will be spun up using a helium gas jet system tangential to the rotor. The optimum spin speed is approximately 170 Hz, which is a compromise among a number of factors[4]. A cross-section of the gyroscope is shown schematically in Figure 4a and a cross-section of the spin-up channel is detailed in Figure 4b. The parting plane of the gyroscope will be oriented such that, after spin-up, the spin axis of the rotor will be nearly parallel to the line of sight to Rigel. During spin-up, adjustments are made to the suspension system to temporarily displace the rotor towards the spinup channel in order to minimize leakage of spinup gas into the gyroscope cavity. Following spinup, the helium gas is turned off and the gyroscope is evacuated to a residual helium partial pressure of less than 10^{-10} torr by a low temperature bakeout method to be described in a later section. This, combined with the benefits afforded by rolling the spacecraft about the line of sight to Rigel (discussed later), ensures that differential damping torques, due to residual gas in the cavity, contribute less than 0.1 milli-arcsecond/year to the absolute drift rate of the gyroscope.

Ground testing of the gyroscopes involves a number of difficulties which are alleviated in orbit. In a 1 g environment, the suspension system must apply an rms voltage greater than 1 kV between the electrodes and the rotor surface, a gap of less than 0.001 inch during spinup, and care must be taken to avoid electrical breakdown. In orbit the gyroscope will normally require suspension voltages much less than 1 V, except during spinup, and

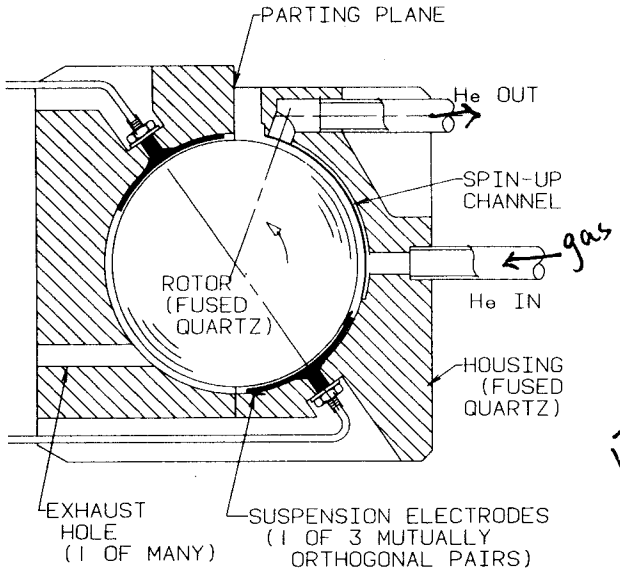

Figure 4a. Cross-section of gyroscope.

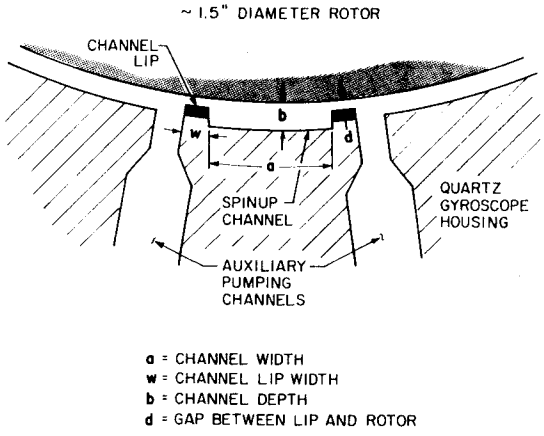

170 Hz

Figure 4b. Cross-section of spinup channel with definition of some important dimensions.

breakdown is less of a problem. In addition, the absolute drift rate of the gyroscope is much less in orbit than during ground tests because the support-dependent torques are smaller by many orders of magnitude.

A most illustrative example of the need to reduce the acceleration on the gyroscope to "near zero" is provided by considering the simplest support-dependent torque: the mass unbalance torque. Consider a rotor that is perfectly spherical but not perfectly homogeneous. When suspended, it is subjected to a torque due to the fact that its center of mass and center of geometry are separated by a distance Δr. One can easily deduce that the drift rate, Ω_u, due to unbalance of this spinning rotor is given by:

$$\Omega_u = \frac{5}{2} \frac{f}{v_s} \frac{\Delta r}{r} \tag{2}$$

where f is the residual acceleration on the rotor, and v_s and r are the rotor peripheral velocity and radius, respectively. A worst case situation is that when $\Delta r/r$ is due to a uniform density gradient, $\delta\rho/\rho$, across the rotor. It can be shown that:

$$\frac{\Delta r}{r} = \frac{3}{8} \frac{\delta\rho}{\rho} \tag{3}$$

By substituting equation (3) into equation (2), and requiring that the contribution of Ω_u be less than 0.1 milli-arcsecond/year, we get:

$$\frac{\delta\rho}{\rho} < \frac{3.6 \times 10^{-14}}{f} \tag{4}$$

On earth, this would require $\delta\rho/\rho < 3.6 \times 10^{-17}$ which is not practically achievable. In orbit, within a drag-free satellite (described later), f is reduced by 10 orders of magnitude so that $\delta\rho/\rho < 3.6 \times 10^{-7}$, a value that is not too much better than that for commercially available fused quartz.

Similar analyses, but of greater complexity, can be applied to determine allowable rotor and suspension electrode asphericity and the allowable rotor coating thickness variation. All of these parameters are expressed as peak-to-valley (p-v) deviations. The derivation of these values can be found elsewhere[8,11,12]. All the major requirements on gyroscope fabrication are collected in Table 1.

Table 1
Major Gyroscope Requirements

Rotor density homogeneity	$\delta\rho/\rho \lesssim 3 \times 10^{-7}$
Asphericity of rotor	$\lesssim 0.8$ μin, p-v
Asphericity of suspension electrodes	$\lesssim 10$ μin, p-v
Rotor coating thickness variation	$\lesssim 0.3$ μin, p-v

Experiment configuration

Recently determined concepts for the overall satellite configuration are discussed in the accompanying paper by Young[5]. The bulk of the spacecraft is the experiment module shown in Figure 5 consisting of a superfluid helium dewar approximately 79 inch in diameter and 120 inch long. Within the dewar is a removable cylindrical high-vacuum chamber called the probe (approx. 10 inch diameter) containing the heart of the experiment, the Quartz Block Assembly/telescope (QBA/telescope). The QBA/telescope is maintained at a stable temperature near 2K and is comprised of four gyroscopes and a drag-free proof mass mounted into a fused quartz block which is bonded, by an optical contacting method, to a fused quartz reference telescope. The dewar is designed for a 1 to 2 year cryogen hold time in space, and embodies

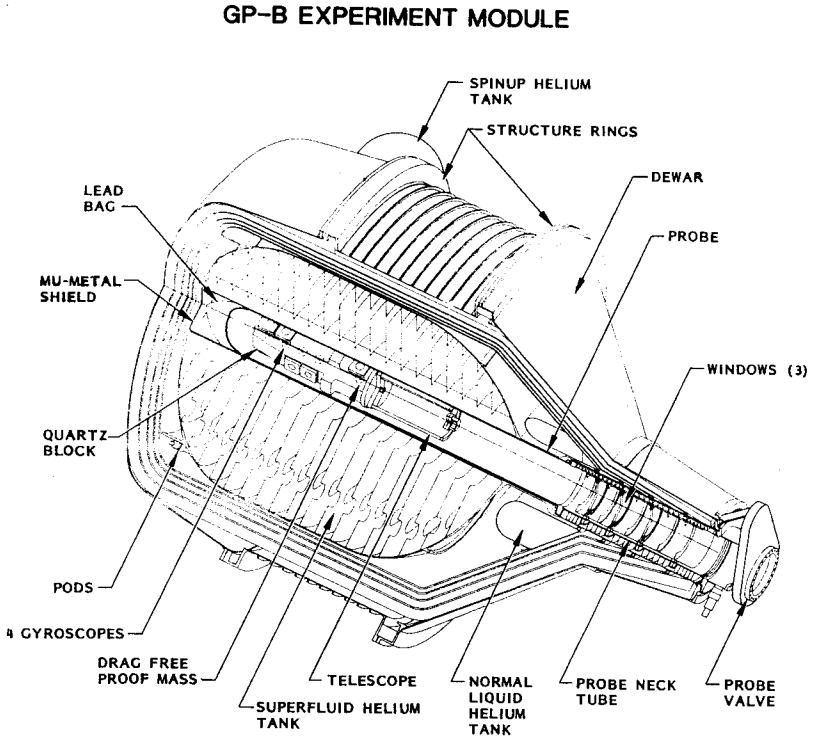

Figure 5. The experiment module showing main elements of the dewar and probe. (Drawing courtesy of Lockheed)

many innovations in space dewar technology. Details of the dewar/probe system are given by Parmley et al.[13], and of the telescope by Everitt et al.[14,8]. The drag free proof mass is located very near the center of mass of the satellite and "floats" in a vacuum cavity. It is therefore unaffected by external disturbances (such as drags from the residual atmosphere) on the spacecraft and follows a near perfect orbit in "free-fall" around the earth. The drift of the proof mass within its housing is precisely sensed to generate signals which control proportional thrusters that utilize the boil-off helium gas from the dewar. These thrusters accelerate the satellite in an appropriate manner so that the proof mass is kept centered within its housing. The residual acceleration on the gyroscopes is thus reduced to less than 10^{-10} g compared to more than 10^{-8} g that would be present, in the absence of the drag-free system, for a satellite at 650 km orbital altitude. The need for this low value of residual acceleration has been previously described. The drag-free system has already ben successfully demonstrated to the 5×10^{-12} g level in the DISCOS controller for the TRIAD satellite[15].

The dewar contains a mu-metal shield which surrounds the probe and provides a portion of the magnetic shielding needed for the experiment. The well is also "lined" with a superconducting lead bag (transition temperature 7.2K) which provides additional magnetic shielding. This combination results in a residual static magnetic field of less than 10^{-7} gauss at the QBA and contributes a major portion of the required overall shielding factor (to externally varying fields) of $\sim 2 \times 10^{-13}$. A superconducting cylindrical layer of niobium surrounding each gyroscope provides additional magnetic shielding and contributes substantially to the overall shielding factor. The static field requirement follows from the need to keep trapped flux in the rotor below a value that could saturate the SQUID system, and the stated shielding factor for varying fields ensures that the variations in the magnetic field of the Earth at the satellite do not masquerade as gyroscope drifts at the 0.1 milliarcsecond/year level. The accompanying paper by Lockhart[10] further describes the superconducting magnetic shielding scheme. This superconducting shielding system demonstrates another major reason for performing the experiment at cryogenic temperatures.

The QBA/telescope is mounted within the probe by bolts which clamp the QBA mounting flange to the probe support structure, as outlined in Figure 6. At the temperatures and vacuum levels utilized in this experiment radiation and gaseous heat conduction between the dewar and the QBA are negligible so that essentially all thermal and mechanical coupling to the QBA is achieved at this interface. The electrical and fluid lines which are needed for the

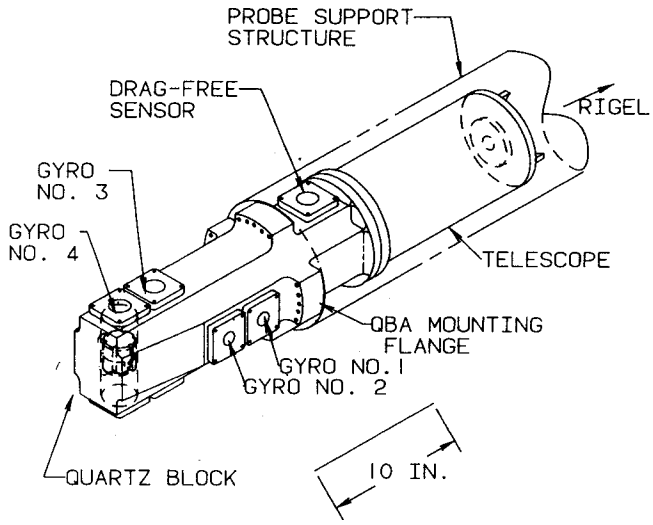

QUARTZ BLOCK ASSEMBLY

Figure 6.

gyroscopes, the drag-free sensor, and numerous other pieces of instrumentation on the QBA are also brought down from the probe neck along the probe support structure. The gyroscopes are mounted in the quartz block as shown such that their parting planes are aligned with the two orthogonal readout directions of the telescope and such that the line forming the intersection of these planes is colinear with the major axis of the QBA. A gyroscope housing assembly is shown in Figure 7. The helium pipes through which the spinup gas flows are attached to one side of the housing. The six suspension cables, which connect to the three pairs of mutually orthogonal electrodes within the gyroscope housing, are shown exiting through the housing retainer. The latter in conjunction with the spacer and index plate form the fused quartz clamping system which is used to hold each gyroscope within the QBA to arcsecond precision. An indication of this is shown in Figure 6 for gyroscope No. 4. Fused quartz is used for the entire QBA/telescope to ensure that there is no differential contraction between major components from room to operating temperatures. Since the QBA/telescope is isolated in a nearly isothermal environment near 2K, it will be largely unaffected by temperature changes elsewhere on the satellite. This provides the gyroscope to telescope stability which is necessary for the experiment and is a further reason for the need to operate at cryogenic temperatures.

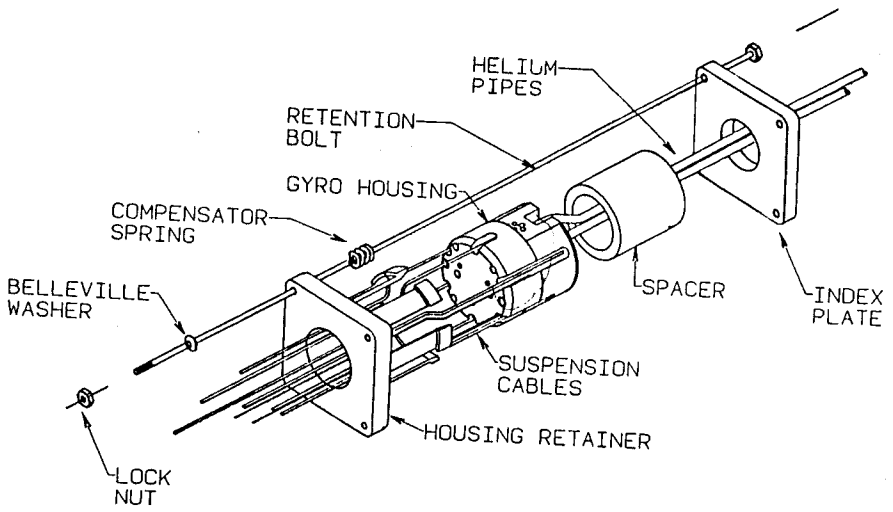

GYRO HOUSING ASSEMBLY
WITH RETENTION HARDWARE

Figure 7.

The gyroscope spin axes will be aligned parallel to the telescope axis and to the line of sight to Rigel, two rotating clockwise and two counter-clockwise. The entire spacecraft is rolled about the line of sight with a 10 minute period which helps to align the spin vectors of the rotors during spinup and serves to average out many of the residual torques on the gyroscopes during the measurements. Further, rolling the spacecraft reduces the effect of 1/f noise in the gyroscope readout system and eliminates errors from null drifts in the gyroscope and telescope readout systems. Rolling the spacecraft (and thus the readout loops) about the line of sight to the reference star causes the total relativistic precession, Ω_T, to manifest itself as a sinusoidal signal of amplitude $\sqrt{\Omega_G^2 + \Omega_M^2}$ whose phase is related to the position of a star in an approximately orthogonal direction to Rigel. This star will be detected by an appropriate "star blipper" located on the side of the spacecraft. A major benefit of roll in this configuration is that it allows determination of the two relativity effects each with four-fold redundancy[3,4].

The present effort is funded by NASA through the Marshall Space Flight Center (MSFC). In the years prior to 1985, work was performed to develop several of the crucial and difficult technologies for gyroscope manufacture, SQUID readout, electrostatic suspension, and magnetic shielding. In March 1985, Stanford University (C.W.F. Everitt, Principal Investigator) was awarded the prime contract for STORE. This Shuttle Test Of the Relativity Experiment will carry a payload, essentially identical to the GP-B experiment module, consisting of the Science Mission dewar with a probe containing a complete QBA and most other internal systems. Within two years after the STORE the payload will be refurbished and upgraded into its complete free-flyer configuration and will be launched as the Science Mission with expected duration to exceed 18 months. After careful consideration, it was determined that STORE, the "engineering test" of GP-B in a low g environment, minimizes the risks of the overall program in a cost effective way because it forms a crucial complement to ground testing and integration of the experiment.

We have formed a team with a group at the Lockheed Research and Development Division, Palo Alto, to carry out the STORE program. The immediate thrust of the program, over approximately the next two years, is twofold: 1) to concentrate on the fabrication and testing of gyroscopes with evolving improvements towards Science Mission requirements; 2) to perform a full size laboratory integration of a Quartz Block Assembly (with two gyroscopes) in a full sized Science Mission-like probe inserted in a laboratory dewar. The former will involve investigations in many technology areas and will utilize the new Gimballed Test Facility at Stanford to characterize the performance of individual gyroscopes; the latter will culminate in the First Integrated System Test (FIST) which will for the first time enable us to evaluate the integrated performance of many of the components of the Relativity Gyroscope Experiment. The balance of this paper will describe specific aspects of the hardware development effort.

Gyroscope development activities

The gyroscope has been described in a previous section and some of its important properties are listed in Table 1. Additional information on gyroscope development is given by Lipa and Keiser[12]. Here we highlight several of the activities that are taking place to design and fabricate gyroscopes which will meet the requirements of the Science Mission. Some of the technologies are already available today, however in some cases further development is required. At the present time, no major obstacles to achieving the necessary gyroscope performance for the STORE or Science Mission are foreseen.

Rotor density homogeneity

The requirement for $\delta\rho/\rho \lesssim 3 \times 10^{-7}$ was previously derived for the worst case assumption of a uniform density gradient across the rotor. The best quality fused quartz commercially available has $\delta\rho/\rho \sim 3 \times 10^{-6}$, inferred from index of refraction variations determined optically, limited by present measurement accuracy. We are working with one manufacturer to develop a special grade of fused quartz with better density uniformity. Because accurate knowledge of density homogeneity is severely limited by current methods of determining index of refraction variations, we are also working with M. Player at the University of Aberdeen, Scotland, where a new instrument is being developed which will use sensitive interferometric techniques in a precisely controlled temperature environment. When completed, the instrument is expected to allow determination of $\delta\rho/\rho$ with an accuracy of $\sim 3 \times 10^{-8}$. We plan to use the instrument to select sufficiently homogeneous material. As an alternative, we may also accept material in which the density variations that do occur are very symmetrically distributed.

Rotor sphericity

The sphericity requirement of $\lesssim 0.8$ μin peak-to-valley is close to being routinely achieved for 1.5 inch diameter fused quartz rotors. The rotors for this program have been supplied to Stanford by MSFC. A special lapping/polishing machine developed by W. Angele[16] uses four lapping elements which contact the quartz rotor in a tetrahedral arrangement. Measurement of sphericity is accomplished with the use of a Talyrond (Rank Taylor Hobson, England) roundness measuring appratus which utilizes a stylus displacement technique. An example of the output from this device around one equator of a recent rotor (S/N 85-10) is shown in Figure 8. The deviations from a perfect circle correspond to $\lesssim 0.7$ μin peak-to-valley. Through the careful work of J. Reed at MSFC we now routinely achieve asphericities less than 1.3 μin and occasionally submicro-inch asphericities. With selection we expect to meet the sphericity requirement.

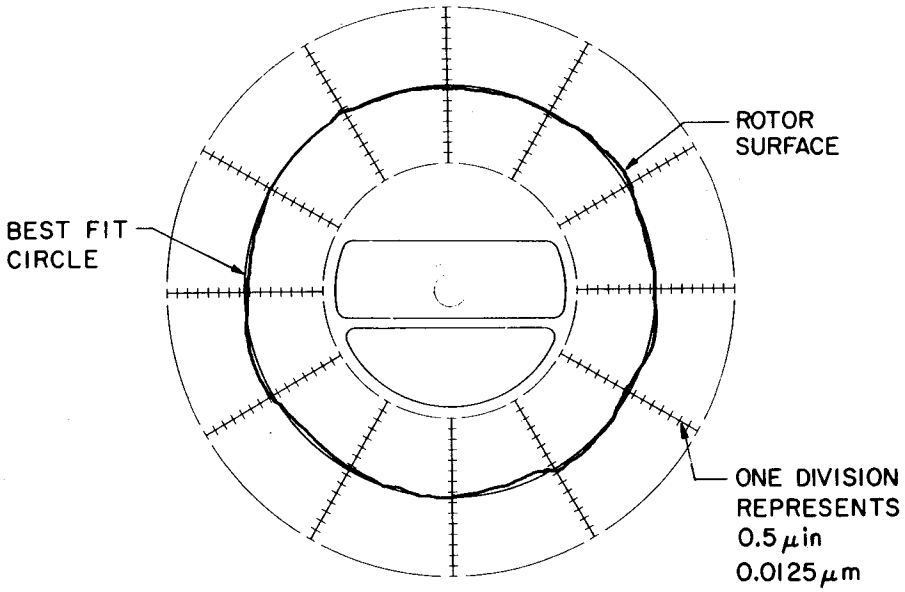

Figure 8. Roundness measurement in one plane for rotor S/N 85-10. Rotor and data supplied by MSFC.

Rotor coating uniformity

The coating of the rotor with niobium represents one of our greatest challenges because it is necessary to make a thin-film coating that is simultaneously superconducting, highly resistant to damage from electrical breakdown during ground testing, and exceedingly uniform. The percentage uniformity depends on the average thickness since the requirement, derived from worst case rotor unbalance considerations, is that the absolute thickness variation not exceed 0.3 μin peak-to-valley. This severe requirement would be somewhat relaxed if we can achieve residual accelerations smaller than the conservatively assumed 10^{-10} g value using drag-free satellite technology. Measurement of film thickness is accomplished by using an apparatus which determines count rates for back-scattered beta-rays impinging on the coated rotor.

We are presently assuming that the average niobium coating thickness must exceed 50 μin to ensure that the layer is sufficiently robust. This would imply a layer thickness non-uniformity of less than 1%, which has as yet not been achieved. Non-uniformities less than 3% have been achieved on rotors coated by P. Peters at MSFC. At Stanford we have constructed a computer controlled rotor manipulator to control the rotation of the rotor in vacuum under a sputter target. This apparatus, shown in Figure 9, allows either discrete depositions on

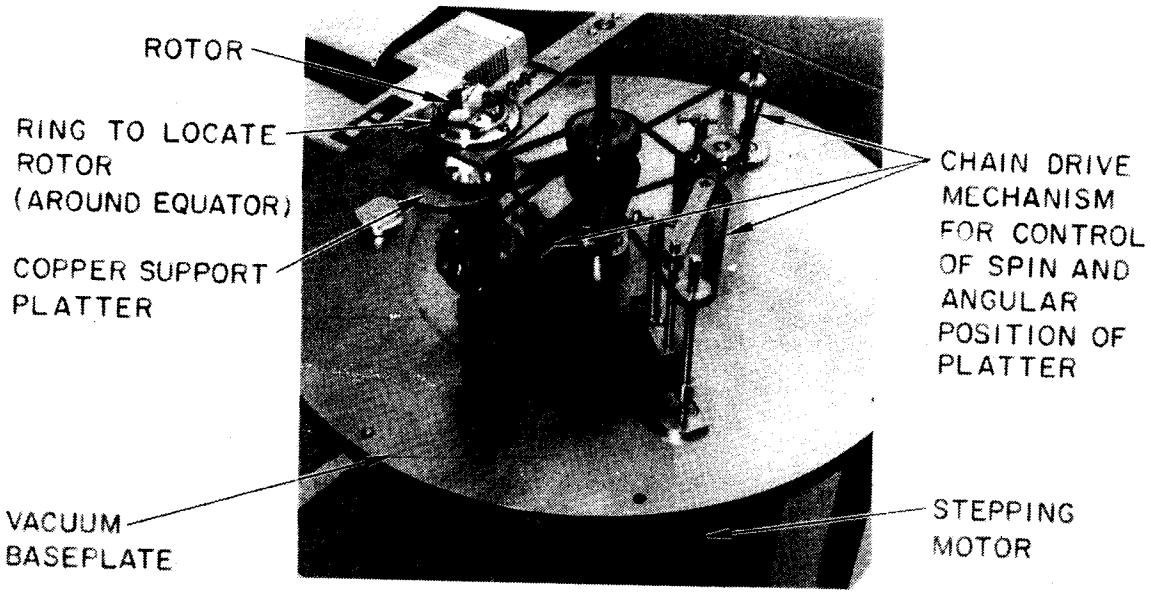

Figure 9. Rotor manipulator for use in sputtering chamber.

the rotor surface or, with appropriate mechanical and software modification, continuous depositions with quasi-random motion of the rotor. We will be investigating the uniformity of niobium coatings produced by a variety of manipulation sequences. Preliminary runs have achieved uniformities sufficient for our present needs and have also revealed a number of needed mechanical improvements. We expect to achieve progressively better uniformity of the coatings by careful optimization of the technique in the future.

Steps have also been taken to ease the requirement for percentage thickness uniformity by making modifications which allow reduction in the average thickness of the rotor coating. These modifications include reducing, from nearly 0.002 inch to ~0.001 inch, the electrode/rotor gap in the latest design for the gyroscope. The effect of the gap reduction is to reduce the magnitude of the necessary suspension voltages. Although the field strength remains unchanged, it is empirically observed that electrical breakdown depends on voltage magnitude in situations similar to the gyroscope geometry. Therefore, by reducing the gap, there is a reduction in the probability of occurrence of electrical breakdown, and when it does occur much lower energy is imparted to the rotor coating. We are also investigating the resistance to breakdown damage for thinner niobium layers. In addition we will pursue other methods of fabricating the superconducting layer that may circumvent the present severe constraints. Finally, it should also be noted that a suitably symmetrical distribution of thickness variations over the rotor surface may also allow a relaxation in the uniformity requirement. This will be studied further as we begin to produce a statistically significant number of rotor coatings in our new facility. In practice, it is likely that

the rotor for use at a particular time will be chosen by a selection process that considers the relative merits of all its properties.

Gyroscope housing fabrication

Since housings have been described in an earlier section, we will only briefly discuss some of the fabrication techniques involved and some areas of concern. The fabrication of the readout loop on the parting plane will be discussed in the next section.

A difficult aspect of housing fabrication is meeting the requirement, listed in Table 1, for the sphericity of the electrodes. Since the electrodes are deposited on the surface of the cavity, the latter must meet an even more severe sphericity requirement. Deviations from sphericity are measured by techniques similar to those used for measuring rotor sphericity. Gyroscope readout considerations determine the additional requirement that the pickup loop, and thus the parting plane of the housing, must lie within 400 μin of the cavity center. We are proceeding with the manufacture of fused quartz housings using two different approaches. In the first, the housing halves are independently machined and hand lapped to try to achieve the required sphericity. The halves are then matched to achieve the overall tolerance required. In the second approach, the housing halves are only rough machined and are delivered as matched pairs pinned together with precision dowels. The housing is opened and a weighted lapping element and appropriate lapping or polishing slurries are inserted into the cavity. The housing is then put back together and tumbled randomly. The heavy lapping element stays near the bottom of the cavity during the tumbling action, and an extremely spherical cavity is formed. A "tumble lap" machine is now being set up at Stanford with help from D. Davidson (Optical Instrument Design, Va.).

Although fused quartz housings provide many advantages for the GP-B gyroscopes, some possible problems exist. For example, the tensile strength of quartz is low and metallic films which form the electrodes may fracture the quartz due to differential contraction as the housing is cooled to cryogenic temperatures. This problem can be avoided by limiting film thicknesses to less than 500 μin, and we are investigating the integrity of suitably thin metallic electrode coatings. Another problem is dielectric heating at the electrode/quartz interface due to power dissipation from the suspension system. This will only be significant in ground tests because of the relatively large voltages required. In addition to narrowing the electrode/rotor gap (discussed above), which reduces the suspension voltage required, the suspension system has been redesigned to operate at 2 kHz instead of 20 kHz. This combination is expected to reduce heating to acceptable levels.

Fabrication of the pick-up loop

As previously described, the readout of the gyroscope will be accomplished with the use of a superconducting pick-up loop which will surround each rotor. This pick-up loop will be deposited on the parting plane surface of one housing half and is presently expected[10] to consist of a continuous coplanar five-turn spiral of niobium consisting of a trace approximately 1000 angstroms thick and 3 μm wide with 3 μm gaps between turns. The inner trace needs to be as close as possible to the rotor for optimum coupling of the magnetic flux due to the London moment. In our previous work, the pickup loop consisted of some turns of niobium wire wound around the outside of the housings; however this will not be sufficient to meet Science Mission requirements. We are investigating loop fabrication by two distinct methods: direct-write photolithography and laser milling.

Direct-write photolithography. In this approach, a source of UV light, with appropriate precision optics and positioning stages, is used to direct-write a pattern onto photoresist which has been deposited onto the parting plane. Most of the technology follows reasonably standard applications of "conventional" UV photolithography. Depending on the choice of photoresist, the pattern which is exposed will either become the desired niobium loop traces or the gaps between the loop traces. This technique has been applied with some preliminary success by P. Peters and his colleagues at MSFC. Care will have to be taken to develop procedures which do not contaminate the niobium film or other surfaces within the housing during steps in the lithography process. We plan to set up a facility at Stanford modelled on the one at MSFC.

Laser milling. An alternative approach to loop fabrication which, in principle, seems straightforward is to deposit the niobium film directly on the parting plane over the area of interest and then mill away unwanted niobium using intense laser radiation of appropriate wavelength. We have been working with XMR Inc. (Santa Clara, CA) which has developed a machine, incorporating a powerful ultraviolet excimer laser with a wavelength of 308 nm, for milling traces in semiconductor microcircuits[17]. The machine is capable of exposing microscopic areas of a surface in its focal plane to short duration pulses of radiation ("burns") with energy densities controllable between 0.1 and 20.0 J/cm^2. The fused quartz substrate upon which the pick-up loop is deposited is transparent to the laser radiation, and thus one does not expect damage to the underlying quartz. To date, samples of approximately 1000 angstrom thick niobium films on thin quartz substrates have been "milled" by this method

using a technique of slightly overlapping the ends of 3 μm × 50 μm laser "burns". Figure 10 shows an SEM picture of an early attempt at this process where a pattern of 3 μm traces was created by "milling" 3 μm gaps. Later work demonstrated improvements in the technique and

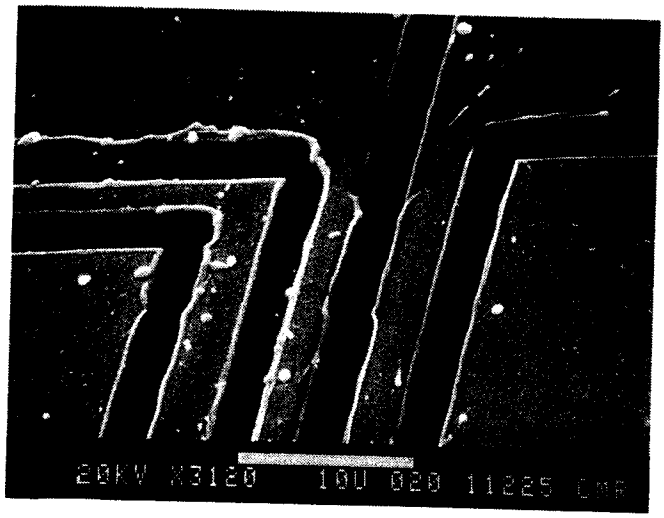

Figure 10. Preliminary result of laser "milling" to produce 3μm traces in a thin niobium sputter film.

resulted in even cleaner looking traces with less debris in the surrounding areas. Surface analysis in the gaps shows that the niobium is removed below levels of detectability. A study of the superconducting properties of traces formed by this method has been undertaken and satisfactory transition temperatures were measured, similar to the transition temperatures of control samples which were not "milled". We plan to proceed with preliminary attempts at loop fabrication in the near future.

Properties of deposited niobium films

To produce the niobium layers needed for rotor coating, as well as for the superconducting readout loop, we developed a deposition facility at Stanford. The system consists of a cryogenically pumped vacuum chamber with a DC magnetron sputtering head and appropriate thickness deposition monitoring equipment. Niobium is susceptible to contamination during deposition and this can dramatically affect its superconducting transition temperature. In addition, the adhesion of thin films of niobium on quartz is dependent on substrate preparation. We undertook a parametric study of film characteristics deposited on flat quartz samples, as a function of various process variables. The adhesion of niobium to quartz is very good and, if the substrates are thoroughly cleaned, pull tests demonstrate an adhesion of approximately 10^4 psi. Comparisons of superconducting transition temperatures as a function of substrate temperature during deposition and niobium deposition rate are shown in Figure 11. The transition temperature is relatively insensitive to substrate temperature for the higher deposition rates, and values are close to 9.2K, which is the expected niobium superconducting transition temperature. At the lowest deposition rate, the partial pressure of contaminants may affect the films as they are forming in a way that is sensitive to temperature. The fact that the higher deposition rates yield films of good quality is convenient for our applications.

Gyroscope spinup method and analysis

The basic concept of spinup has been described in a previous section. Here we discuss the spinup analysis which has been developed to predict the spinup characteristics of the gyroscope under various conditions. The gyroscope rotor is spun up with a helium gas jet which flows tangentially to the rotor surface and which is contained by a channel built into the gyroscope housing[18,19]. The essential features of the spinup channel are shown in Figure 4. The spinup gas enters the spinup inlet, passes through the spinup channel and then leaves through the spinup exhaust. Located on the perimeter of the spinup channel is a lip which serves to reduce the leakage of spinup gas into the rest of the housing. Just outside the lip is an auxiliary pumping channel which conducts the gas to 11 pumping holes through which the leakage gas is pumped. Since the probe valve at the neck is open during spinup, the leakage gas will be pumped to space and the pressure at the gyroscope will be limited by the conduction characteristics of the probe. During spinup the rotor is displaced towards the single spinup channel by adjustment of the suspension system. This provides

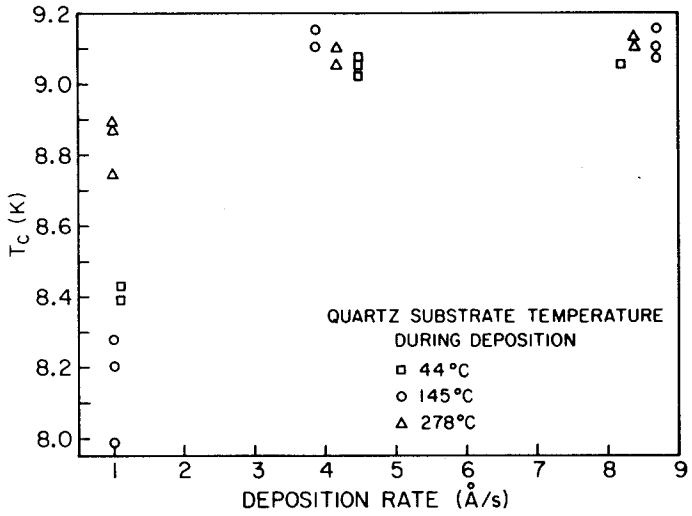

Figure 11. Superconducting transition temperature versus deposition rate and substrate temperature for 1000 angstrom thick niobium sputter films.

the advantage of a small gap (about 200 μin) during spinup to reduce gas leakage and allows a larger gap during normal operation to increase clearance between the housing and the rotor. Helium gas of about 30 torr is then applied to the spinup inlet and pumped from the spinup exhaust. The gas flowing through the spinup channel torques the rotor causing it to spin up. The spin speed of the rotor is limited by viscous gas damping between the rotor and the spinup lip and by molecular gas damping over the area outside of the spinup channel and lip. After spinup the rotor is moved back to the housing center. The gyroscope is then baked out at low temperature following a procedure described below. Final operating pressure of the gyroscope is less than 10^{-10} torr which reduces differential damping torques from the residual gas to "near zero".

The low temperature bakeout procedure is analogous to high vacuum bakeout used to "clean up" vacuum systems at several hundred degrees centigrade. After the spinup gas is turned off, the gyroscope is pumped for a while by the ambient vacuum of space since the probe valve is still open. For several hours a heater will keep the temperature of the gyroscope slightly elevated at approximately 6K. This facilitates desorption of helium from the gyroscope's surfaces. The probe valve will then be closed and the heater turned off. When the gyroscope cools to its normal operating temperature, the pressure will be below 10^{-10} torr. This technique has been demonstrated by Turneaure et al.[20] in a laboratory simulation which achieved an ultimate pressure of $\sim 5 \times 10^{-11}$ torr.

The principal requirement of the gas spinup system is that the gyroscope reaches a spin speed of 170 Hz. Other design requirements are that the helium gas pressure between the rotor and suspension electrodes, as well as outside the housing be maintained at pressures below the threshold of avalanche breakdown, that the spinup time be less than 2 hours (for convenience), and that the effective acceleration on the rotor caused by the gas pressure in the channel be less than 0.3 g.

An integrated analysis program has been developed to study the gyroscope spinup. This program includes the calculation of the rotor torque produced by the gas flowing in the channel, the viscous drag between the channel lip and rotor, the gas leakage over the lip into the auxiliary channel, the pressure along the auxiliary channel due to the gas leakage, pumping through the auxiliary pumping holes, the molecular drag between the housing and rotor outside of the spinup channel, and the pressure outside of the housing. The asymptotic spin speed as a function of spinup inlet pressure and the gap between the spinup lip and rotor is shown in Figure 12 for the parameter values given. The spin speed requirement of 170 Hz can be met for a range of inlet pressures and gaps. Table 2 presents the results of a specific calculation which shows that all of the requirements can be met simultaneously. The value of leakage flow rate shown in the table is being used to determine aspects of probe design. In particular, the probe must have sufficient conductance for helium so that the pressure at the gyroscopes will not exceed approximately 5×10^{-4} torr, the pressure at which avalanche breakdown may occur.

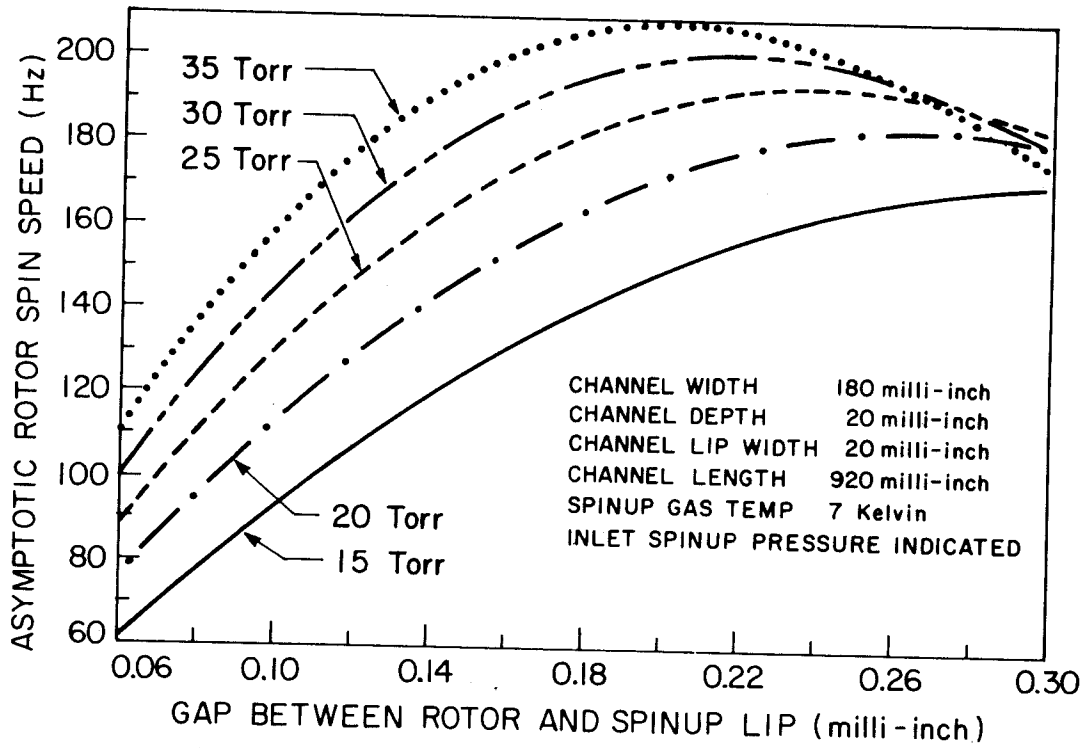

Figure 12. Results of spinup analysis. See text and Figure 4b for description and definitions.

Table 2
Example of Spinup Characteristics

Gap between lip & rotor	0.185 milli-inch
Inlet spinup pressure	25 torr
Asymptotic spin speed	183 Hz
Spinup time to 170 Hz	40 min
Leakage flow rate	140 μg/s
Eff. acceleration on rotor	0.3 g

Gyroscope testing facilities

A major ongoing effort at Stanford has been the testing of gyroscope assemblies.[12] Since 1976, ground testing of gyroscopes has taken place both at room temperature and in the ultra-low field gyroscope test facility (also known as the Low Temperature Test Facility). Collectively, gyroscopes have been operated for over 10,000 hours at cryogenic temperatures. On numerous occasions gyroscopes have been spun up in a very low magnetic field (a few microgauss) environment facilitated by an expanded lead bag maintained for five years below its superconducting transition temperature. The concept of London moment readout has been demonstrated and tested in this facility.

This Low Temperature Facility has some limitations, however. Ultra-low pressures of 10^{-10} torr can not be achieved because of the probe design, and gyroscope drift rate investigation is limited because the orientation of the housing is fixed in the laboratory and cannot be changed during a particular test. To enhance our testing capability, we have completed the first phase of construction of our Gimballed Test Facility which allows the gyroscope assembly to be rolled and oriented in a chosen direction during operation. This is accomplished by mounting the liquid helium dewar on a precision air bearing turntable on a gimbal mount. The setup shown in Figure 13 is tilted parallel to the Earth's spin axis and is attached to the turbo-pump system needed to exhaust the helium leakage gas during spinup. Because of the load constraints of the turntable, we cannot use a dewar long enough to accommodate an ultra-low field lead bag shield. Magnetic shielding is accomplished by mu-metal only, providing residual fields at the gyroscope between 10 and 100 micro-gauss. This results in trapped flux levels in the rotor which exceed the field of the London moment at low spin speeds. A trapped flux readout gives sufficient precision for gyroscope characterization tests and also has the advantage of allowing precise studies of rotor polhoding.

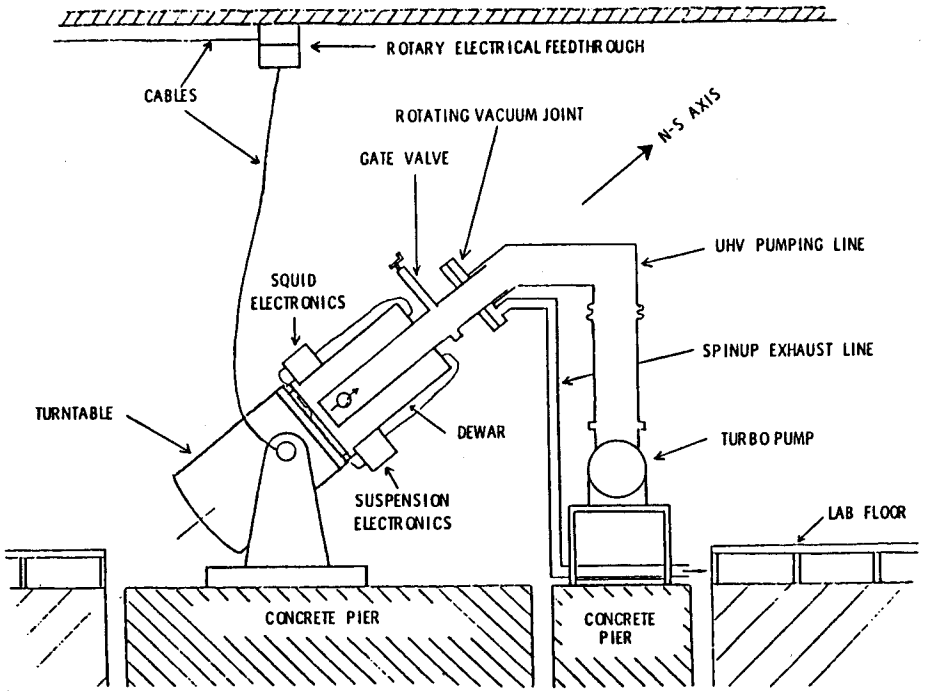

Figure 13. Schematic of new gyroscope test facility (Gimballed Test Facility) for evaluation of the performance of gyroscopes.

In addition, the trapped flux enables us to easily observe rotor spin speed and direction since the flux lines are fixed with respect to the rotor and not the spin direction. Rolling the gyroscope housing during spinup aids in the alignment of rotor spin vector and during normal operation serves to average out many torques on the rotor. The roll capability has not yet beem implemented in the Gimballed Test Facility because we must complete the design and construction of the rotating vacuum coupler, appropriate electrical slip rings, and modification to the dewar for vapor/liquid phase separation at all roll angles.

Because the dewar can only accommodate a short probe, it had to be designed with careful consideration of all thermal, mechanical and vacuum constraints. Figure 14 is a schematic representation of the probe within the dewar, and Figure 15 is a picture of the probe prior to its insertion into the dewar. The vacuum can containing the gyroscope must be kept (except during gyroscope spinup) at ultra-high vacuum, while the well in the dewar which surrounds the probe, is maintained at a less stringent high-vacuum level. Thermal communication between the probe and the dewar is accomplished through four thermal/mechanical connections (in the form of expansion rings) at the dewar and probe neck assemblies. This is done in a manner similar to that of the Science Mission design. An additional connection is made at the base of the vacuum can. The temperature of the gyroscope during stable operation will be about 4.5K and during spinup the incoming helium gas will be cooled by passing it through heat exchangers on the probe resulting in a controllable gas temperature at the gyroscope of ~7K, still safely below the niobium superconducting transition temperature. This will provide spinup conditions similar to those of the Science Mission and will allow parametric tests of spinup as a function of spinup gas pressure and temperature. The heat exchanger locations in the neck are cooled by a series of shields through which the cold helium boil-off gas from the liquid reservoir passes before being vented. Figure 14 also indicates measured temperatures along the probe in various locations, for normal conditions and when additional heat is purposely dissipated in the liquid helium reservoir. The latter measurements are shown in parentheses. The dissipation of extra heat into the reservoir accelerates helium boil-off causing temperatures along the neck to be depressed. This technique facilitates enhanced leakage gas conduction during spinup, and may be similarly utilized in the Science Mission[13].

In summary, the Gimballed Gyroscope Facility will be used for a series of single gyroscope tests beginning with our current rotors, housings, and readout systems, and evolving over the course of several years to characterization tests of flight gyroscopes. Results of these tests, when compared to theoretical predictions from information on rotor and housing

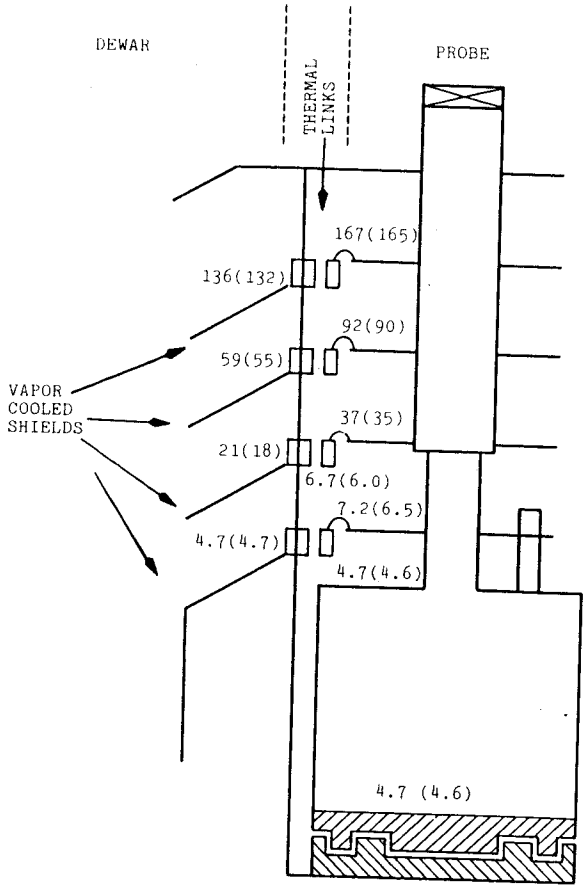

Figure 14. Schematic representation of the Gimballed Test Facility probe in the dewar. Numbers are temperatures (in Kelvin) at various locations. Those in parentheses are for an additional 100 mW heat dissipation in liquid helium reservoir.

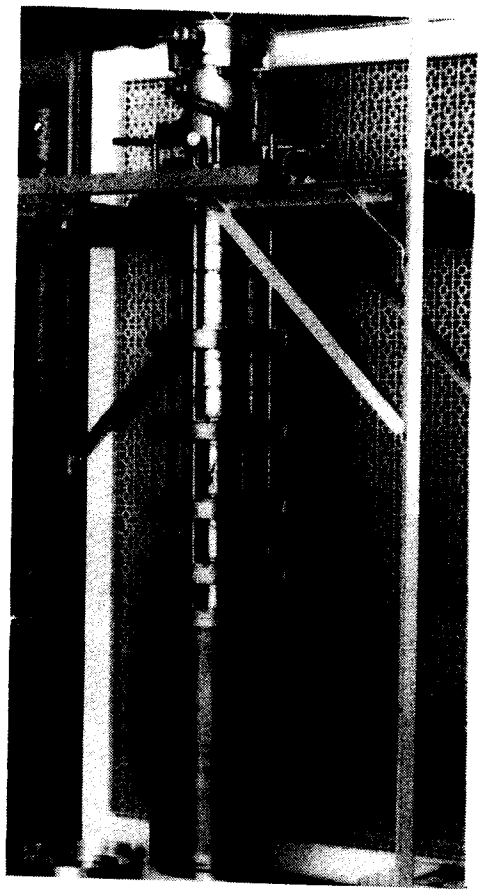

Figure 15. Photograph of Gimballed Test Facility probe on clean bench prior to insertion into dewar. Note correspondence of the four thermal/mechanical expansion rings (links) to those shown in Figure 14.

sphericity, rotor homogeneity and coating uniformity, spinup gas temperature and pressure, to name but a few, will enhance our understanding of gyroscope performance and requirements. The first test, Gimballed Gyroscope Test-A, will use a rotor with a coating thickness variation of approximately 3 μin peak-to-valley. When this gyroscope is spun up to 50 Hz, within a few degrees of the Earth's rotation axis (without housing roll), we expect to measure a drift rate on the order of 4 deg/hr. In later tests, which will include rolling the dewar with a ten minute period about an axis parallel to the Earth's axis, we expect (with a flight quality gyroscope) to verify a drift rate approximately 40 times smaller.

Full size integration and tests

A major thrust of the current work on GP-B is to demonstrate as soon as possible the capability to integrate and test a full size probe with a full size quartz block assembly (QBA). This will culminate in the First Integrated System Test (FIST). One major task is to fabricate the quartz block and gyroscopes, and develop the techniques to assemble and align the QBA. Although the FIST is a ground test and will not involve a vibration test, we are designing as many components as possible with Science Mission considerations in mind to provide heritage to future flight articles. In particular, the QBA for FIST will be prototypical of the QBA we expect to use on the Science Mission. The present design has been subjected to an analysis to determine stress levels under conservative launch conditions. The results of this analysis will be described below and will be followed by a brief description of the FIST.

Stress analysis of the QBA/telescope design

The QBA/telescope is shown in Figure 6 and a general description has been provided in a previous section. This assembly is approximately 39 inches long with about 23 inches for the length of the QBA and has a 9.4 inch diameter cruciform mounting flange. The mass of the QBA/telescope will be approximately 76 lbs with center of mass very close to the mounting plane along the telescope axis. The QBA is attached to the probe support structure (indicated with broken lines) at the QBA mounting flange by a series of bolts. This will hold the QBA/telescope in precise alignment with the probe/dewar system and will provide the thermal link to maintain the experiment at a stable temperature near 2K. During launch, the QBA/telescope will be subjected to vibration levels which must not be allowed to damage the structure. An estimate of loads during Shuttle launch has been made by Lockheed and is very conservatively determined to be a maximum of 15 g at the QBA mounting flange with only significant frequency components below 200 Hz. The stress levels allowable in fused quartz depend on the margin of safety that is desired. We conservatively choose the maximum stress level allowable to be 750 psi.

The cruciform shape of the QBA provides bending strength. The location of the mounting flange near the center of mass of the QBA/telescope ensures that translational accelerations do not apply large moments at the mounting plane. An additional advantage of attaching the QBA/telescope to the support structure in a single plane is that bending of the QBA is minimized and thus the readout loops in the gyroscopes remain accurately oriented with respect to the telescope. Compressional stress, produced by the fasteners at the mounting flange, is expected to be largely limited to the flange volume, although more analysis is needed on this aspect. We have made the flange thick (2 inch) to distribute loads evenly near the mounting plane.

The QBA/telescope structure was modelled using 767 nodes and three-dimensional isoparametric brick elements. A dynamic analysis was performed which determined that the lowest free-free bending mode for the QBA/telescope is above 700 Hz. Since launch loads are not expected to have large frequency components above 200 Hz, a quasistatic structural analysis is justified. In this analysis, 15 g loads are applied independently in four directions at the mounting plane: three directions transverse to, and one aligned with, the main (telescope) axis. Stress levels below 350 psi are calculated for loads along each of the four directions. The actual stress will be higher than this because of additonal stress induced by the fasteners on the mounting structure; however it appears that the total will be safely below the present maximum design level.

First Integrated System Test - FIST

The purpose of FIST is to demonstrate compatibility amongst the GP-B technologies in a full size, integrated form. It will hopefully also verify analyses that are used to design many of the components of the probe and QBA. Finally, in proceeding to FIST, we will develop the integration and alignment techniques necessary for the STORE and Science Mission and will establish the Stanford Ground Test and Integration Facility (GTIF) which will be used throughout the rest of the GP-B program.

The QBA for FIST will have gyroscope assemblies installed in two positions only. The QBA will be integrated into a full size probe which will be designed and fabricated to be nearly identical to the Science Mission probe in its thermal and gas conductance characteristics. The probe will be integrated into an engineering development dewar which will have a superfluid hold time of 2 to 4 weeks. It will have mu-metal shielding and a full size superconducting lead bag in its well. Thermal/mechanical interfaces to the probe at the neck will closely mimic those of the Science Mission design concept. The dewar will be tilted parallel to the Earth's spin axis, in a similar fashion to that for the Gimballed Test Facility (see Figure 13). Because of cost constraints the dewar will not be rolled about its axis. This will mean that gyroscope performance will not be as good as in the Gimballed Test Facility; however, the primary aim of FIST is to determine the integrated performance and interaction of components.

New facilities will be specially developed at both Stanford and Lockheed to accomplish the various tasks of: insertion of the lead bag into the dewar; assembly of the QBA; integration of the QBA into the probe; and insertion of the probe into the dewar. Electronics for the suspension system and SQUID readout will be laboratory units presently in existence or under development. Appropriate vacuum pumping and fluid supplies will also be provided. Data acquisition will be automated wherever possible but will involve mostly laboratory type and commercially available equipment.

The major goals of FIST are:

a) to develop the many cleanroom handling and integration procedures for the full size system,

b) to verify design of the probe and QBA in a parametric series of spinup tests, with close attention given to thermal and gas conduction performance. To this end the system will be thoroughly instrumented with heaters and temperature sensors.

c) to fully investigate the magnetic shielding properties of all the various shields, including an evaluation of any crosstalk between gyroscopes. We will also investigate techniques to purge magnetic flux from rotors, local superconducting shields, pick-up loops, and SQUIDs. This involves temporarily heating the particular item to a temperature just above its superconducting transition temperature.

d) to evaluate SQUID performance and any sensitivity to possible sources of instrument-generated EMI.

e) to verify that gyroscope drift performance is as expected for FIST conditions and to compare results with those previously determined in the Gimballed Test Facility.

f) to verify that we can indeed achieve stable high vacuum conditions of $\lesssim 10^{-10}$ torr at the gyroscopes after low temperature bakeout.

In summary, the FIST will establish confidence in Science Mission concepts and will provide data for flight hardware designs. We will have developed the skills and the precision fixtures and metrology equipment to integrate flight units. We will have begun to establish the integration facilities at both Stanford and Lockheed to be used throughout the STORE program, and we will have developed the interface procedures (both technical and managerial) that are necessary for a program of the magnitude of GP-B.

Acknowledgments

The authors wish to thank C. W. F. Everitt for his encouragement and suggestions in preparing this paper. In addition to those mentioned in the text, we acknowledge the efforts of J. Neighbors and R. Potter of MSFC and members of the Lockheed team. The present work on the GP-B STORE program is supported by NASA under contract number NAS8-36125.

References

1. Schiff, L. I., Proc. Nat. Acad. Sci. 46, 871 (1960).
2. Schiff, L. I., Phys. Rev. Lett. 4, 215 (1960).
3. Everitt, C. W. F., "The Stanford Relativity Gyroscope Experiment (A): History and Overview," Near Zero: New Frontiers of Physics (W. H. Freeman, New York, to be published).
4. Everitt, C. W. F., ed., The GP-B Relativity Gyroscope Experiment, Stanford University document (August 1984).
5. Young, L. S., "Systems Engineering for the Gravity Probe-B Program," presented at this conference, SPIE Proceedings 619 (1986).
6. Van Patten, R. A., DiEsposti, R., and Breakwell, J. V., "Ultrahigh resolution science data extraction for the Gravity Probe-B gyro and telescope," presented at this conference, SPIE Proceedings 619 (1986).
7. Van Patten, R. A., "Flight Suspension for the Relativity Gyro," Proceedings of the Third Marcel Grosmann meeting on General Relativity, Hu Ning, ed. (Science Press and North-Holland Publishing Company, 1983).
8. Everitt, C. W. F., ed., Report on a program to develop a gyro test of General Relativity in a satellite and associated control technology, W. W. Hansen Lab., Stanford University (June 1980).
9. London, F., Superfluids Vol. 1: Macroscopic Theory of Superconductivity, 83 (John Wiley, New York, 1953).
10. Lockhart, J. M. "SQUID readout and ultralow magnetic fields for the Gravity Probe-B," presented at this conference, SPIE Proceedings 619 (1986).
11. Keiser, G. M., Suspension torques on a gimballed electrostatically supported gyroscope and requirements on the gyroscopes and spacecraft for the Relativity Gyroscope Experiment, Stanford University document (February 1985).
12. Lipa, J. A., and Keiser, G. M., "The Stanford Relativity Gyroscope Experiment (B): Gyroscope Development," Near Zero: New Frontiers of Physics (W. H. Freeman, New York, to be published).
13. Parmley, R. T., Goodman, J., Regelbrugge, M., and Yan, S., "Gravity Probe-B Dewar/Probe Concept," presented at this conference, SPIE Proceedings 619 (1986).
14. Everitt, C. W. F., Davidson, D. E., and Van Patten, R. A., "Cryogenic star-tracking telescope for Gravity Probe-B," presented at this conference, SPIE Proceedings 619 (1986).
15. The staffs of the Space Dept. of the Johns Hopkins University Applied Physics Laboratory, and the Guidance and Control Laboratory of Stanford, "A satellite freed of all but gravitational forces: TRIAD I," J. Spacecraft, 11, No. 9 (September 1974).
16. Angele, W., "Finishing high precision quartz balls," Prec. Engr., 2, 119 (1980).

17. Leung, C., McCarthy, M., and Scott, J., "Selective submicron trace cutting and thin film removal using an ultraviolet laser," Proceedings of International Symposium for Testing and Failure Analysis 1985, Long Beach, CA (1985).
18. Bracken, T. D., and Everitt, C. W. F., in Advances in Cryogenic Engineering, Vol. 13, Timmerhaus, K. D., ed., 168 (Plenum Press, NY, 1968).
19. Karr, G. A., Hendricks, J. B., and Lipa, J. A., Physica, 107B, 21 (1981).
20. Turneaure, J. P., Cornell, E. A., Levine, P. D., and Lipa, J. A., "The Stanford Relativity Gyroscope Experiment (D): Ultrahigh Vacuum Techniques for the Experiment," Near Zero: New Frontiers of Physics (W. H. Freeman, NY, to be published).